Hydrogenated Ring-Opened Polynorbornene: A Highly Crystalline Atactic Polymer

Li-Bong W. Lee[†] and Richard A. Register*

Department of Chemical Engineering, Princeton University, Princeton, New Jersey 08544-5263

Received September 26, 2004; Revised Manuscript Received November 26, 2004

ABSTRACT: Ring-opening metathesis polymerization (ROMP) of norbornene with most catalysts produces a polymer with an atactic placement of the cyclopentylene rings, yet partial hydrogenation of this polymer is known to yield a crystalline product. We report here a facile catalytic route to saturate polynorbornene (PN); fully hydrogenated polynorbornene (hPN) is highly crystalline, with an equilibrium melting point estimated as 156 °C. The crystal lattice is monoclinic, with parameters $a = 6.936$ Å, $b = 9.596$ Å, $c = 12.420$ Å, and $\beta = 130.7°$ at room temperature, indicating nearly complete extension of the hPN backbone within the unit cell. The material remains highly crystalline until the melting point is reached, but near 105 °C, the crystal structure transforms to one characterized by substantial rotational disorder of the hPN chains about their axes, while retaining substantial translational order.

Introduction

Norbornene (bicyclo[2.2.1]hept-2-ene), a bicyclic olefin, is a versatile monomer. It can be polymerized to high molecular weights in at least two ways: either through the double bond while retaining both rings[1] or through ring-opening metathesis polymerization (ROMP), opening one ring and retaining the unsaturation.[2,3] This paper is concerned with ROMP polynorbornene (poly(vinylene-1,3-cyclopentylene)), referred to simply as polynorbornene (PN) hereafter. PN is produced commercially under the trade name of Norsorex by Atofina, using a heterogeneous catalyst ($RuCl_3$) which yields a high molecular weight, polydisperse polymer.[4] The mixed *cis*/*trans* configuration of the double bond produces an amorphous material with a glass transition temperature[5] of 35 °C. During the past two decades, the development of homogeneous ROMP initiators which yield "living" polymerizations[3,6] has paved the way for producing near-monodisperse PN and for the incorporation of PN blocks into well-defined block copolymers.[3,7]

The unsaturated character of PN makes it highly susceptible to oxidative degradation,[4] a problem which can be circumvented by hydrogenating the polymer. Several investigators have attempted to hydrogenate PN, either catalytically (with Wilkinson's catalyst[4,8,9] or $HRh(CO)(PPh_3)_3$;[4] $RuCl_3$,[4] $RuCl_2(PPh_3)_3$,[4] or $RuCl_2(PCy_3)(CHOEt)$;[10] PtO_2,[8] Co/Al,[4] or Ni[4]) or through the noncatalytic diimide method.[4,11] All reported that PN was difficult to saturate, and frequently incomplete (or zero) saturation was achieved, though some procedures[4,10,11] produced sufficient saturation to note that hydrogenated PN (hPN) was crystalline, with properties greatly different from the amorphous unsaturated PN. This finding is remarkable since hPN is atactic,[12] as discussed further below. Moreover, the facile polymerization of norbornene with living ROMP initiators opens the door to new well-defined block copolymers containing a crystallizable block, after hydrogenation.[13]

Here, we present a facile catalytic route for the complete hydrogenation of PN to hPN, using PN prepared with a living ROMP catalyst. Fully saturated hPN is a highly crystalline polymer, with an equilibrium melting point of approximately 156 °C. The lattice parameters for hPN are determined by fiber X-ray diffraction; at room temperature, the structure shows the three-dimensional order normally associated with stereoregular polymers, but near 105 °C, the structure transforms to one characterized by significant rotational disorder.

Experimental Section

ROMP. Polymerizations were performed in flame-dried glassware under a nitrogen atmosphere (<1 ppm of O_2, H_2O) in an Innovative Technology glovebox. Toluene used as the solvent for polymerizations was dried over sodium benzophenone ketyl, degassed by freeze−pump−thaw cycles, and vacuum-transferred prior to use. Norbornene (Aldrich, 99%) and PMe_3 (Aldrich, 97%) were dried over sodium, degassed, and vacuum-transferred (at 50 °C for norbornene, a solid at ambient). The ROMP initiator, 2,6-diisopropylphenylimidoneophylidenemolybdenum(VI) bis(*tert*-butoxide), a "Schrock-type" catalyst, was used as received (Strem Chemicals), as was the terminating agent, benzaldehyde (Aldrich, 99.5%). Polymerizations were conducted at room temperature, at 0.04 g monomer/mL solution, with a monomer:initiator ratio calculated to produce the desired molecular weight at complete monomer conversion. A 5:1 molar ratio of PMe_3:initiator was employed for consistency with earlier work, where it was found that PMe_3 suppresses the formation of a subsidiary amount of very high molecular weight polymer.[14] This level of PMe_3 also slows the polymerization by a factor of 3, but the reaction still proceeds to >99.9% conversion within the 1 h allotted for polymerization,[15] after which the reaction was terminated with 100 equiv of benzaldehyde. The polymer was isolated by twice precipitating into a 2:1 methanol:acetone mixture and vacuum-drying.

Hydrogenation. Polymers were dissolved at 2 wt % in an 80/20 mixture of cyclohexane/tetrahydrofuran and hydrogenated at 100 °C and 400−600 psig of H_2 (BOC Gases, 99.999%). The catalyst employed was 5 wt % reduced Pd on $CaCO_3$ (Strem, used as received),[16] typically added at a 2:1 wt ratio of catalyst (including support) to polymer. Hydrogenations were typically carried out for 48 h; progress of the reaction was periodically monitored by infrared spectrometry (Nicolet 730). Trans units (965 cm^{-1}) hydrogenated more slowly than *cis* units (738 cm^{-1}), as previously reported;[11] hydrogenations were continued until the band at 965 cm^{-1} was no longer

[†] Present address: ExxonMobil Upstream Research Co., P.O. Box 2189, Houston, TX 77252.

* Author for correspondence: e-mail register@princeton.edu.

10.1021/ma048013a CCC: $30.25
Published on Web 01/21/2005

detectable, which we estimate to correspond to a maximum of 0.25% residual unsaturation. The catalyst was separated from the solution by hot filtration, and the polymer was isolated by precipitation into methanol and dried in a vacuum oven. The crystalline nature of hPN precludes posthydrogenation characterization by room temperature gel permeation chromatography; however, poly(ethylidene norbornene) saturated in our laboratory under identical conditions shows no backbone rearrangements,[14] and poly(ethylidene norbornene) exhibits even poorer thermooxidative stability than polynorbornene. Consequently, we expect that no molecular weight changes occurred upon hydrogenation.

Characterization. Polymer molecular weights and polydispersity indices were determined by gel permeation chromatography in toluene,[14] with columns calibrated against polystyrene standards. The true molecular weight is obtained by dividing the apparent molecular weight by a factor[17] of 2.2 for polynorbornene. Though several polymers of different molecular weights and narrow distributions were synthesized,[18] all the data in this paper were acquired on a single polymer with a true M_n = 60 kg/mol (61 kg/mol after hydrogenation) and M_w/M_n = 1.11.

^{1}H NMR spectra of PN were acquired in C_6D_6 at room temperature on a General Electric QE 300. ^{13}C NMR spectra of hPN were acquired in C_6D_{12} at 65 °C on a Varian Inova 500, following the protocol of Al-Samak et al.[12] Differential scanning calorimetry (DSC) data were acquired with a Perkin-Elmer DSC-7 calibrated with indium and mercury, scanning at 10 °C/min. Pressure−volume−temperature measurements were performed by Dr. Gregory T. Dee of DuPont Central Research & Development using a Gnomix PVT apparatus.[19] Standard PVT runs were performed; at a fixed temperature (5 °C increments), pressures are increased in 10 MPa increments from 0 to 200 MPa. The specific volumes at zero gauge pressure were employed for analysis; the room temperature density is measured via an autopycnometer.

Powder X-ray diffraction measurements employed Cu Kα radiation and a Philips-Norelco wide range goniometer operating in reflection with an Advanced Metals Research graphite crystal focusing monochromator and were conducted on a film of hPN compression-molded and cooled slowly to room temperature. For fiber X-ray diffraction, fibers of hPN were drawn manually by heating a small quantity of material on a hot plate to just above its melting point, grabbing the melt with tweezers, and pulling rapidly. Fibers were aligned together into a bundle sufficiently large to cover the X-ray beam. Fiber diffraction measurements employed an evacuated pinhole camera (Statton camera, W.H. Warhus, 500 μm pinholes), equipped with hot stage, using Cu Kα X-rays from a planar graphite monochromator. Diffraction patterns were recorded on image plates (Kodak) read with a Molecular Dynamics PhosphorImager SI, providing a digital version of the diffraction pattern directly. The positions of the reflections in the diffraction patterns were calibrated by working finely ground NaCl (a = 5.6402 Å[20]) into the fiber bundle after completion of all the measurements reported herein and remeasuring the room temperature diffraction pattern.

Results and Discussion

ROMP can produce four distinct configurations of the norbornene (1,3-cyclopentylenevinylene) repeat unit, as shown in Figure 1. Though the cyclopentylene rings themselves necessarily have a *cis* configuration (retained from the monomer), the vinylene moiety possesses *cis*/*trans* isomerism, and sequential cyclopentylene rings may exist in either *meso* or *racemo* dyads. The *cis*/*trans* isomerism of the double bond is eliminated upon saturation, as shown in Figure 1, but the two dyad configurations are retained. Al-Samak et al.[12] investigated PN prepared with five different ROMP initiators and found that none was capable of producing highly stereospecific addition (all <90% *m* or *r* dyads); $RuCl_3$, the commercial catalyst, produced atactic polymer (*m*:*r* ratio essentially 1:1). Recently, Hayano et al.[10] have described a nonliving ROMP catalyst which seems to produce more stereoregular PN, though no *m*:*r* ratio or similar characterization was reported due to the polymer's insolubility.

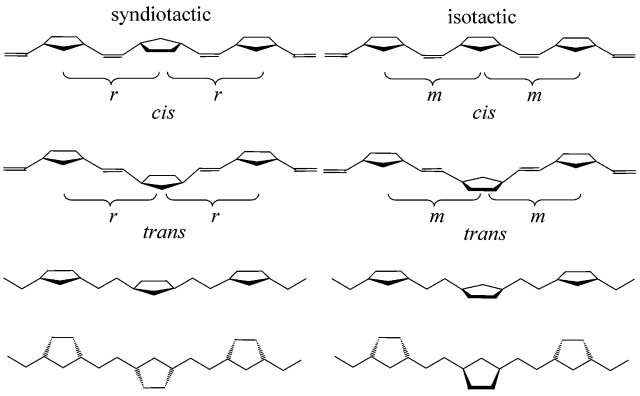

Figure 1. Illustration of syndiotactic (left) and isotactic (right) PN triads showing both *cis* (top line) and *trans* (middle line) configurations of the vinylene moiety. The third and fourth lines show the corresponding hPN triads, where the *cis*/*trans* isomerism of the vinylene unit is eliminated by hydrogenation but the distinction between *m* and *r* dyads remains. The third and fourth lines in each column represent the same structure, simply rotated about the chain axis.

^{1}H NMR revealed that our unsaturated PN had a 54/46 *cis*/*trans* ratio but cannot reveal the *m*:*r* ratio, which was probed by ^{13}C NMR on fully saturated hPN following the method of Al-Samak et al.[12] Figure 2 shows the relevant regions of the spectrum. Peak deconvolutions indicate an *m*:*r* ratio of 0.8:1 and an *mm*:*mr*/*rm*:*rr* ratio of 1:2.3:0.8; these are within the deconvolution error of the values expected for a Bernoullian dyad distribution, indicating that PN obtained with this Schrock-type initiator is atactic, in common with PN obtained from $RuCl_3$[12] and several other[10,12] catalysts.

DSC heating and cooling traces for hPN are shown in Figure 3. The heating trace, taken after previously cooling the specimen from the melt at 10 °C/min, shows a peak melting temperature T_m = 143 °C, with a total enthalpy of fusion ΔH = 65.4 J/g. A subsidiary peak near 105 °C is observed in both the DSC heating and cooling traces, with an enthalpy constituting 5% of the total, whose origin is discussed further below. The values of T_m and ΔH exceed those reported for similarly atactic hPN, "fully saturated" via the diimide method (136 °C)[4] or by catalytic hydrogenation at 160 °C over $RuCl_2(PCy_3)(CHOEt)$ (136 °C and 46 J/g),[10] demonstrating a higher degree of saturation in our polymer. Cataldo[11] employed the diimide method coupled with scrupulous investigation of the resultant hPN by infrared spectroscopy and found that a polymer with T_m = 140.8 °C and ΔH = 58.7 J/g (slightly below our values) still had detectable residual unsaturation. Moreover, the hydrogenated polymer contained sulfinic acid groups attached to the backbone,[11] a common side reaction in the diimide process;[16] the diimide process can also produce significant cleavage of the polymer chain.[21] All of these problems are avoided by hydrogenation over Pd/$CaCO_3$.

The equilibrium melting temperature T_m^0 of hPN was estimated via a Hoffman−Weeks extrapolation[22] by crystallizing a specimen isothermally in the DSC at various temperatures T_c and then scanning upward to record the peak melting temperature T_m. Figure 4 shows

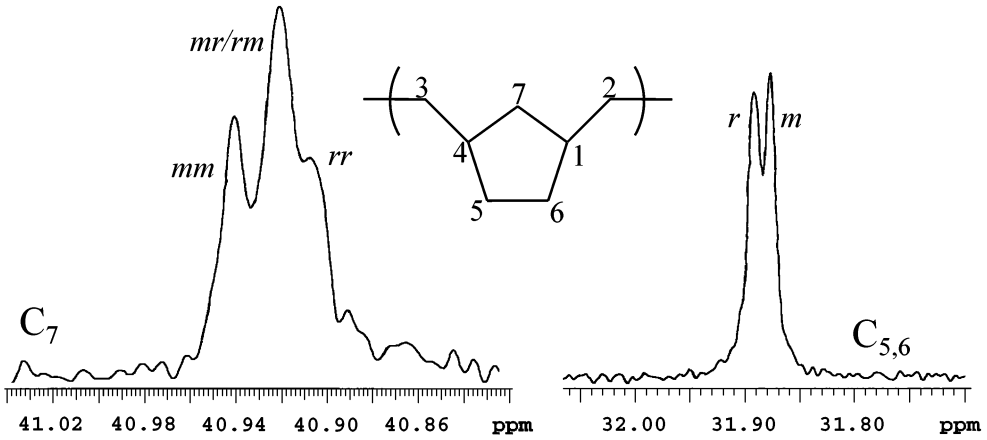

Figure 2. Selected regions of the ^{13}C NMR spectrum of hPN in C_6D_{12} solution at 65 °C. Carbons are numbered according to Al-Samak et al.,[12] following the schematic in the center; peaks corresponding to *m* and *r* dyads are labeled at right and those corresponding to *mm*, *mr*/*rm*, and *rr* triads at left.

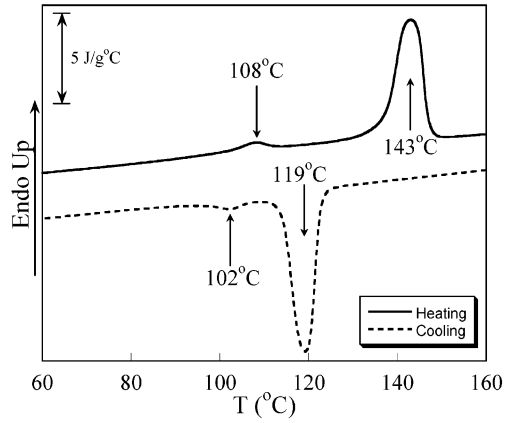

Figure 3. DSC second heating and cooling traces of hPN (M_n = 61 kg/mol) at 10 °C/min.

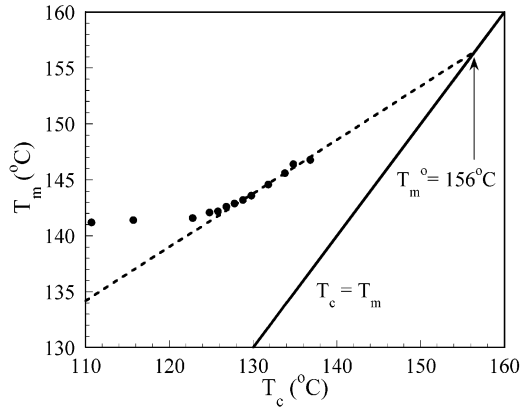

Figure 4. Hoffman−Weeks plot for hPN, yielding an estimate of the equilibrium melting point T_m^0 = 156 °C.

the results; below 125 °C, truly isothermal crystallizations are impossible due to the rapid crystallization of hPN (see DSC cooling trace in Figure 3). Fitting the data from T_c = 129−137 °C to a straight line and extrapolating to $T_m = T_c$ yields T_m^0 = 156 °C. Heating rate effects produce T_m values approximately 3 °C higher when scanning at 10 °C/min (data of Figure 4) vs 1 °C/min, leading to a modest overestimate of T_m^0; however, a larger source of uncertainty is the Hoffman−Weeks approach itself, which Marand and co-workers have recently shown to underestimate T_m^0 by an amount considerably larger than 3 °C in typical cases.[23,24] Our

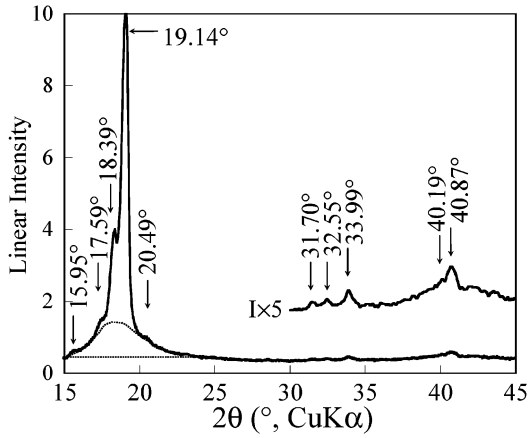

Figure 5. Powder diffraction pattern taken on compression-molded and slow-cooled specimen of hPN, with peak positions labeled. Amorphous scattering indicated by dotted curve.

value of T_m^0 = 156 °C for hPN should thus be considered a first estimate, best refined by direct crystal thickness measurements and an extrapolation according to the Gibbs−Thomson equation.[25]

The powder X-ray diffraction pattern of our hPN is shown in Figure 5, indicating a high-crystallinity material. The weight fraction crystallinity w_c was approximately evaluated from the integrated areas of the amorphous hump and the crystalline peaks, yielding $w_c \approx 0.76$. Thus, fully saturated hPN is comparable in both melting point and degree of crystallinity to other common polyolefins, such as linear polyethylene and isotactic polypropylene.

Figure 6 presents the room temperature fiber X-ray diffraction pattern, which exhibits several sharp high-intensity arcs; the azimuthal intensity distribution of the arcs is influenced by imperfect alignment of fibers within the bundle, and only the radial position and azimuthal position corresponding to the maximum intensity along each arc are analyzed further. All observed reflections could be satisfactorily indexed by a monoclinic lattice, with parameters a = 6.936 Å, b = 9.596 Å, c = 12.420 Å, and β = 130.7°; as shown in Table 1, all calculated and observed reflections agree within 0.4% in Bragg spacing d and within 2° in azimuthal position, measured as the azimuthal angle σ from the equator to the reflection; these small deviations correspond to our measurement uncertainty.[18] On the

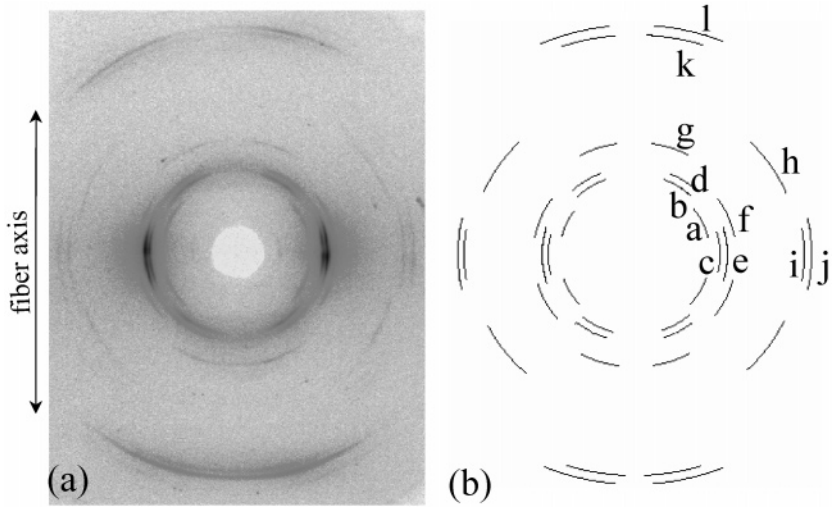

Figure 6. (a) Fiber X-ray diffraction pattern of hPN at room temperature. (b) Schematic of diffraction pattern, with reflections labeled. Fiber axis vertical.

Table 1. Reflection Indexing for HPN Fiber Diffraction Pattern at Room Temperature; Calculations Based on a Monoclinic Lattice, with a = 6.936 Å, b = 9.596 Å, c = 12.420 Å, and β = 130.7°

reflection	index	d, expt (Å)	σ, expt (deg)	d, calc (Å)	σ, calc (deg)
a	$\bar{1}11$	5.594	27	5.593	27
b	$\bar{1}12$	5.026	55	5.034	55
c	020	4.790	0	4.798	0
d	002	4.708	51	4.708	50
e	110	4.618	0	4.611	0
f	021	4.283	21	4.275	20
g	$\bar{1}13$	3.793	71	3.793	69
h	$\bar{1}32$	2.825	27	2.814	28
i	130	2.726	0	2.732	0
j	$\bar{2}00$	2.621	0	2.629	0
k	$\bar{1}15$	2.248	74	2.252	75
l	$\bar{2}25$	2.206	72	2.200	71

assumption of four ethylene-1,3-cyclopentylene repeats per unit cell (discussed further below), this translates to a crystal density of 1.0191 g/cm^3, in good agreement with the measured bulk density of 0.9954 g/cm^3 for the semicrystalline hPN at room temperature.

At this point, we pause to note that such a high degree of crystallinity—indeed, *any* crystallinity—is unexpected for an atactic polymer. There are, of course, exceptions. First, when the substitutents on the stereogenic carbons are of similar size, *m* and *r* dyads can cocrystallize in a common lattice via an isomorphous substitution; poly(vinyl fluoride), a highly crystalline polymer which nevertheless contains both *regio* and *stereo* defects, is a classic example.[26,27] However, only very small size differences between the substituents can be tolerated for an isomorphous substitution; for example, if the substituent is increased from F to Cl to yield poly(vinyl chloride), only a very small degree of crystallinity is developed, through selective crystallization of the longest syndiotactic sequences.[28,29] Second, a strong specific interaction between chains, such as hydrogen bonding, can stabilize the regular packing required for crystallization, even though the atactic nature of the polymer necessarily means that not all the repeat units can orient in such a way as to participate in this interaction. Poly(vinyl alcohol) is a classic example.[30,31] However, hPN does not correspond to either of these cases; it is a saturated hydrocarbon polymer with only dispersive interactions between chains, and the units that are

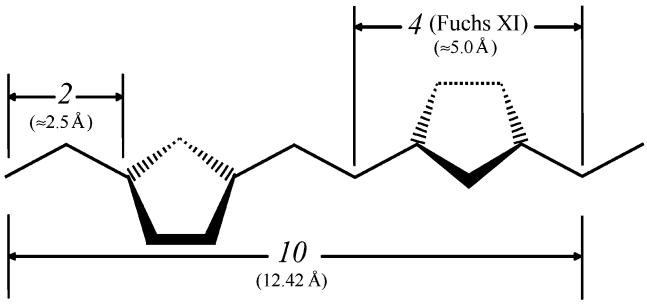

Figure 7. Schematic of a representative hPN dyad (*m* dyad shown), with the cyclopentylene rings in the Fuchs XI conformation and the ethylene sequences in the *trans* zigzag conformation. The measured *c*-axis dimension of 12.42 Å corresponds to 10 backbone carbons; note the quasi-period of 2.5 Å, which corresponds to both the length of the ethylene sequences and half the span between methylene carbons attached to the cyclopentyl ring in the Fuchs XI conformation.

responsible for the stereoirregularity (see Figure 1) are cyclopentylene rings, which can hardly be considered small. Indeed, the most closely related polymer discussed previously in the literature would seem to be poly(methylene-1,3-cyclopentylene), PMCP, which differs from hPN by having a methylene unit, rather than an ethylene unit, connecting the cyclopentylene rings. An atactic PMCP with an 86% *cis* configuration of the cyclopentylene rings (hPN has 100% *cis* configuration of the rings, as noted above) *is* highly crystalline on the basis of the relative crystalline and amorphous peak areas in the powder diffraction pattern but shows only two reflections, both on the equator,[32] indicating poor three-dimensional order, unlike the fiber patterns for hPN (Figure 6). Indeed, PMCP chains of different stereoregularities all show hexagonal packing of extended chains, without true 3D order.[32] It is unclear whether this qualitative difference between PMCP and hPN results from the inability to achieve 100% *cis*-cyclopentylene rings in PMCP (which is prepared by a ring-closing polymerization of 1,5-hexadiene) or from the different numbers of methylene units separating the cyclopentylene rings; in hPN, the even number of methylene units produces opposite orientations of the cyclopentylene rings when the backbone is extended to the *trans* zigzag conformation (see Figure 7), producing a larger and more anisotropic chain cross section than in PMCP. It is worth noting that unsaturated PN

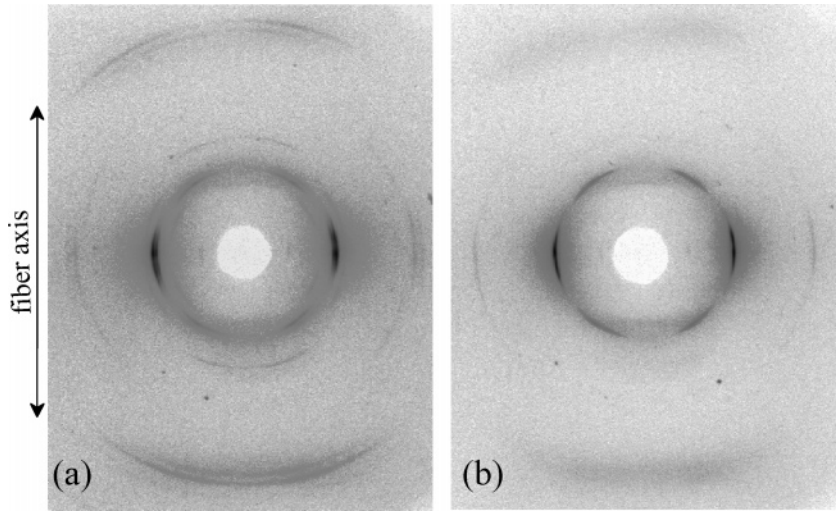

Figure 8. Fiber X-ray diffraction patterns of hPN at (a) 95 and (b) 120 °C.

develops a low level of crystallinity when stretched,[5,33] despite the mixed *cis*/*trans* configuration of the vinylene moiety, though the diffraction pattern does not resemble that in Figure 6.

Further insight into the hPN crystal structure can be obtained by considering a representative sequence and conformation, as shown schematically in Figure 7. Here, we consider an *m* dyad, with the cyclopentylene ring in its lowest energy conformation, the so-called "Fuchs XI" conformation.[34] The cyclopentylene ring is of course not planar, and the potential energy differences around the pseudorotation circuit are rather small;[34,35] the ability of the cyclopentylene ring to alter its conformation may facilitate crystallization in this atactic polymer. Fuchs XI is an "envelope" conformation of the ring; in *cis*-1,3-dimethylcyclopentane, the Fuchs XI conformation maximizes the distance between the substituent methyl carbons[35] at 5.0 Å. For polyethylene, the fiber repeat distance,[36] corresponding to two methylene carbons in the *trans* zigzag conformation, is 2.543 Å. The two-mer sequence illustrated in Figure 7, with 10 backbone carbons, can thus be envisioned very simply as consisting of two *cis*-1,3-dimethylcyclopentane units in the Fuchs XI conformation spliced to two methylene units in the *trans* zigzag conformation, for a total length of 2(5.0) + 2.543 = 12.5 Å. The measured *c*-axis dimension for hPN (12.42 Å) is entirely consistent with this value; note that at this level of approximation, both *m* and *r* dyads have equivalent lengths, though the slightly smaller value of *c* observed experimentally doubtless reflects torsional distortions of the backbone induced by hPN's atactic character.

Inspection of Figure 7 reveals the origin of the unusually strong fifth-layer-line reflections in hPN, which are clearly visible in Figure 6: though the repeat unit (for the hypothetical fully isotactic or syndiotactic polymer) contains 10 backbone carbons, there is a two-backbone-carbon quasi-repeat, since the length of the ethylene sequence and the distance between substituted carbons on the cyclopentylene ring are both nearly 2.5 Å. A similar situation occurs for poly(tetramethylene oxide), PTMO, which crystallizes in a *trans* zigzag conformation;[37−39] the fiber repeat comprises two mers (10 backbone atoms: eight carbons and two oxygens). Though the C−O and C−C bond lengths (and associated bond angles) are not identical, they are sufficiently similar for PTMO to show unusually strong fifth-layer-line reflections. The PTMO crystal structure belongs to the *C*2/*c* space group.

The stereoirregular nature of hPN will result in variations between unit cells in a way which would be poorly described with a Debye−Waller factor, since the atomic positions will likely show multiple preferred locations according to the sequence distribution, rather than having positions symmetrically distributed about a central maximum. While this prevents us from determining a full solution to the hPN crystal structure, it is worth noting that the observed reflections for hPN (Table 1) are consistent with the extinction rules[40] for the *C*2/*c* space group (only $h + k$ = even allowed; $h0l$ allowed only when l = even). Additionally, the *C*2/*c* space group mandates two elements per unit cell, confirming the assumption made from the bulk density that the unit cell contains four hPN mers.

hPN Crystal Structure at Elevated Temperatures. As noted above, DSC heating and cooling traces show a subsidiary peak around 105 °C, well below the primary melting temperature. This transition is visible in the specific volume vs temperature curve as well;[18] the specific volume of bulk hPN is 0.5% larger at 105 °C than a smooth extrapolation of the curve from 40 to 75 °C would suggest. An obvious explanation for this DSC peak and specific volume change would be the melting of a small population of thinner, less perfect secondary crystals. However, this interpretation is not consistent with the relatively small heating/cooling hysteresis observed for this peak in Figure 3. An alternative possibility is a structural change within the hPN crystals below T_m, which we investigated through fiber diffraction at elevated temperatures.

Figure 8 shows the fiber diffraction patterns for the same hPN bundle as Figure 6, but at 95 and 120 °C. The 95 °C pattern is identical to that at room temperature, with a small change in the lattice parameters: a = 6.934 Å, b = 9.625 Å, c = 12.364 Å, and β = 129.3°. The 0.5% contraction of the *c*-axis dimension between 23 and 95 °C is consistent with increased torsional distortions of the backbone. By contrast, the 120 °C pattern is quite different. Most of the reflections visible at room temperature and 95 °C are absent; only three clear reflections remain, while the fifth layer line has become a diffuse blur. With only three reflections available, the diffraction pattern does not permit unambiguous determination of the lattice type and pa-

rameters, but it is instructive to note that two of the sharp reflections lie on the equator, with d spacings of 4.777 and 2.758 Å; the third lies off the equator, at $\sigma = 55°$ and $d = 4.901$ Å. The positions of the three reflections thus correspond roughly to those of "pairs" of reflections in the room temperature and 95 °C patterns ((110) + (020); (200) + (130); ($\bar{1}$12) + (002)).

The ratio of d spacings for the two equatorial reflections equals $\sqrt{3}$, suggesting a hexagonal packing of the hPN chains perpendicular to their axes with $a_{hex} = 5.516$ Å. Indeed, transitions from a low-temperature crystal structure having true three-dimensional order to a high-temperature hexagonal phase, where there is rotational disorder about the chain axis, are well-known for other polymers: a classic example is *trans*-1,4-polybutadiene,[41,42] which transforms from monoclinic to hexagonal at 76 °C. However, the third reflection observed for hPN at 120 °C, which lies neither on the equator nor on the meridian and which has a larger d spacing than either equatorial reflection, rules out a hexagonal unit cell. If instead we assume that the structure remains monoclinic at 120 °C and assign the off-axis reflection to be the (002), this yields a value of $c \sin \beta = 9.802$ Å at 120 °C. The measured azimuthal angle $\sigma = 55°$ is satisfied with $\beta = 126°$ and $c = 12.1$ Å, though this separation of $c \sin \beta$ into its constituent factors is highly sensitive to the value of σ, whose precision is limited by the azimuthal spreading of the arcs. A hexagonal packing of the chains normal to their axes (with $a_{hex} = 5.516$ Å) is achieved in a monoclinic β unit cell with $\beta = 126°$ when $a = 6.82$ Å and $b = 9.55$ Å.

So, while the very limited number of reflections precludes precise determination of the lattice constants, the structure at 120 °C is consistent with a monoclinic structure having substantial rotational disorder of the hPN chains. This rotational disorder, which we speculate is favored by the stereoirregular nature of hPN (as in PMCP[32]), leads to simple hexagonal packing transverse to the chain axes. Nevertheless, a high degree of translational order is preserved, as indicated by the persistence of sharp (002) spots and a diffuse but quite visible fifth layer line; consequently, the high-temperature structure is not truly hexagonal (which would correspond to $\beta = 90°$). This decrease in packing regularity is reflected in the subsidiary endotherm observed by DSC in the same temperature range. However, the material remains highly crystalline until T_m is reached, as evidenced by the low intensity of the amorphous halo in Figure 8b and the small magnitude of the subsidiary DSC endotherm relative to the principal one. Measurements of the mechanical behavior of hPN at elevated temperatures are currently underway.

Conclusions

In common with polynorbornenes prepared via several nonliving ROMP catalysts, PN produced with a living Schrock-type initiator is atactic. Nonetheless, hPN prepared therefrom is highly crystalline, with $w_c \approx 0.76$ estimated from powder diffraction, and possessing an equilibrium melting point of approximately 156 °C. Fiber diffraction patterns taken below 100 °C reveal a monoclinic crystal with good three-dimensional order and a c-axis dimension indicating nearly complete extension of the backbone. But near 105 °C, 40 °C below the melting point, the degree of order within the crystal decreases abruptly, reflecting rotational disorder about the chain axes. Nonetheless, hPN remains highly crystalline up to its melting point. Using living ROMP catalysts followed by hydrogenation, block copolymers containing a highly crystalline hPN block can now be synthesized.[13]

Acknowledgment. This work was supported by the Polymers Program of the National Science Foundation (DMR-0220236). The authors thank Dr. Gregory T. Dee of DuPont Central Research & Development for the density measurements.

References and Notes

(1) Patil, A. O.; Zushma, S.; Stibrany, R. T.; Rucker, S. P.; Wheeler, L. M. *J. Polym. Sci., Part A: Polym. Chem.* **2003**, *41*, 2095.
(2) Ivin, K. J.; Mol, J. C. *Olefin Metathesis and Metathesis Polymerization*; Academic Press: London, 1997.
(3) Grubbs, R. H., Ed. *Handbook of Metathesis;* Wiley-VCH: Weinheim, 2003; Vol. 3.
(4) Abboud, W.; Revillon, A.; Guyot, A. *New Polym. Mater.* **1989**, *1*, 155.
(5) Sakurai, K.; Takahashi, T. *J. Appl. Polym. Sci.* **1989**, *38*, 1191.
(6) Schrock, R. R. *Acc. Chem. Res.* **1990**, *23*, 158.
(7) Saunders, R. S.; Cohen, R. E.; Schrock, R. R. *Macromolecules* **1991**, *24*, 5599.
(8) Ivin, K. J.; Laverty, D. T.; Rooney, J. J. *Makromol. Chem.* **1977**, *178*, 1545.
(9) Ivin, K. J.; Laverty, D. T.; Rooney, J. J.; Watt, P. *Pays-Bas* **1977**, *96*, M54.
(10) Hayano, S.; Kurakata, H.; Tsunogae, Y.; Nakayama, Y.; Sato, Y.; Yasuda, H. *Macromolecules* **2003**, *36*, 7422.
(11) Cataldo, F. *Polym. Int.* **1994**, *34*, 49.
(12) Al-Samak, B.; Amir-Ebrahimi, V.; Carvill, A. G.; Hamilton, J. G.; Rooney, J. J. *Polym. Int.* **1996**, *41*, 85.
(13) Lee, L.-B. W.; Register, R. A. *Macromolecules* **2004**, *37*, 7278.
(14) Trzaska, S. T.; Lee, L.-B. W.; Register, R. A. *Macromolecules* **2000**, *33*, 9215.
(15) Hatjopoulos, J. D.; Register, R. A. *ACS PMSE Proc.* **2004**, *91*, 971.
(16) Rachapudy, H.; Smith, G. G.; Raju, V. R.; Graessley, W. W. *J. Polym. Sci., Polym. Phys. Ed.* **1979**, *17*, 1211.
(17) Schrock, R. R.; Feldman, J.; Cannizzo, L. F.; Grubbs, R. H. *Macromolecules* **1987**, *20*, 1169.
(18) Lee, L.-B. W. Ph.D. Thesis, Princeton University, 2004.
(19) Zoller, P.; Bolli, P.; Pahud, V.; Ackermann, H. *Rev. Sci. Instrum.* **1976**, *47*, 948.
(20) Donnay, J. D. H., Ondik, H. M., Eds. *Crystal Data: Determinative Tables*, 3rd ed.; National Bureau of Standards: Washington, DC, 1973; Vol. 2.
(21) Hahn, S. F. *J. Polym. Sci., Part A: Polym. Chem.* **1992**, *30*, 397.
(22) Hoffman, J. D.; Weeks, J. J. *J. Res. Natl. Bur. Stand.* **1962**, *66A*, 13.
(23) Marand, H.; Xu, J.; Srinivas, S. *Macromolecules* **1998**, *31*, 8219.
(24) Xu, J.; Srinivas, S.; Marand, H.; Agarwal, P. *Macromolecules* **1998**, *31*, 8230.
(25) Al-Hussein, M.; Strobl, G. *Macromolecules* **2002**, *35*, 1672.
(26) Natta, G.; Bassi, I. W.; Allegra, G. *Atti Accad. Nazl. Lincei, Cl. Sci. Fis. Mater. Nat., Rend.* **1961**, *31*, 350.
(27) Lando, J. B.; Hanes, M. D. *Macromolecules* **1995**, *28*, 1142.
(28) Burleigh, P. H. *J. Am. Chem. Soc.* **1960**, *82*, 749.
(29) Guerrero, S. J.; Keller, A.; Soni, P. L.; Geil, P. H. *J. Polym. Sci., Polym. Phys. Ed.* **1980**, *18*, 1533.
(30) Bunn, C. W. *Nature (London)* **1948**, *161*, 929.
(31) Cho, J. D.; Lyoo, W. S.; Chvalun, S. N.; Blackwell, J. *Macromolecules* **1999**, *32*, 6236.
(32) Ruiz de Ballesteros, O.; Venditto, V.; Auriemma, F.; Guerra, G.; Resconi, L.; Waymouth, R.; Mogstad, A.-L. *Macromolecules* **1995**, *28*, 2383.
(33) Sakurai, K.; Kashiwagi, T.; Takahashi, T. *J. Appl. Polym. Sci.* **1993**, *47*, 937.
(34) Fuchs, B.; Wechsler, P. S. *Tetrahedron* **1977**, *33*, 57.
(35) Ruiz de Ballesteros, O.; Cavallo, L.; Auriemma, F.; Guerra, G. *Macromolecules* **1995**, *28*, 7355.

(36) Quirk, R. P.; Alsamarraie, M. A. A. In *Polymer Handbook*, 3rd ed.; Brandrup, J., Immergut, E. H., Eds.; John Wiley & Sons: New York, 1989; p V/15.
(37) Imada, K.; Miyakawa, T.; Chatani, Y.; Tadokoro, H.; Murahashi, S. *Makromol. Chem.* **1965**, *83*, 113.
(38) Cesari, M.; Perego, G.; Mazzei, A. *Makromol. Chem.* **1965**, *83*, 196.
(39) Kobayashi, S.; Tadokoro, H.; Chatani, Y. *Makromol. Chem.* **1968**, *112*, 225.
(40) Henry, N. F. M., Lonsdale, K., Eds. *International Tables for X-Ray Crystallography*; Kynoch Press: Birmingham, UK, 1969; Vol. 1.
(41) Iwayanagi, S.; Sakurai, I.; Sakurai, T.; Seto, T. *J. Macromol. Sci., Phys.* **1968**, *2*, 163.
(42) Suehiro, K.; Takayanaki, M. *J. Macromol. Sci., Phys.* **1970**, *4*, 39.

MA048013A